Open Archive TOULOUSE Archive Ouverte (OATAO)

OATAO is an open access repository that collects the work of Toulouse researchers and makes it freely available over the web where possible.

Modelling multi-scale microstructures with combined Boolean random sets: A practical contribution

Florent S. Bourgeois [a,*], *Geoffrey J. Lyman* [b], *Frédéric Courteille* [a]

[a] *Université de Toulouse, Laboratoire de Génie Chimique, UMR 5503, ENSIACET/INPT, 4 allée Emile Monso, 31432 Toulouse Cedex 4, France*
[b] *Materials Sampling & Consulting Pty Ltd, 17 Diosma St, Bellbowrie, Qld 4070, Australia*

ABSTRACT

Boolean random sets are versatile tools to match morphological and topological properties of real structures of materials and particulate systems. Moreover, they can be combined in any number of ways to produce an even wider range of structures that cover a range of scales of microstructures through intersection and union. Based on well-established theory of Boolean random sets, this work provides scientists and engineers with simple and readily applicable results for matching combinations of Boolean random sets to observed microstructures. Once calibrated, such models yield straightforward three-dimensional simulation of materials, a powerful aid for investigating microstructure property relationships. Application of the proposed results to a real case situation yield convincing realisations of the observed microstructure in two and three dimensions.

Keywords: Microstructure modelling; Boolean random set

1. Introduction

The smaller the scales at which we observe materials, the more aware we become of the overwhelmingly multi-scale nature of materials. Materials formed using nanoparticles, for instance, which are expected to modify profoundly the technological world, are bound to exhibit several structural scales due to the high surface reactivity of nanoparticles (Jeulin and Moreau, 2005). It is to be expected that the complex interactions between these scales will affect the macroscopic properties of nanomaterials to a great extent. In order to optimally tailor the properties of processes and materials, engineers and scientists need to correlate statistical and topological properties of multi-scale structures with the observed macroscopic behaviour of the structures in service (Jeulin, 2005).

The study of multi-scale materials invariably requires that we describe them with appropriate morphological models. There is however an infinity of multi-scale models from which to choose which makes model selection challenging. Multi-scale models are easy to create, starting from a basis of Poisson point processes. The simple superposition of two Poisson point processes with different intensities, yields a rich family of multi-scale processes. Such models have in fact received a great deal of attention in the literature and are classified as a Poisson cluster model (Cressie, 1993). Special cases of Poisson cluster models, also referred to as Boolean cluster models (Rataj and Saxl, 1997) have been studied extensively. As examples, one may quote spatial Cox processes (Møller, 2005), the Neyman–Scott process (Diggle, 1983), the Strauss process (Cuzick and Edwards, 1990) and the Matern process (Stoyan, 1992). The reader is invited to consult one of the numerous textbooks that present clustered point processes (e.g. Illian et al., 2008; Cressie, 1993). For materials structure modelling we replace the points by actual particles, such as convex sets.

Multi-scale structures can be described and modelled with Boolean random sets (BRS). Starting with a single Poisson point process, and replacing each point with a convex grain with known Lebesgue measure (area or volume), yields a BRS (Serra, 1982), a special class of random closed sets (RACS) (Matheron, 1975). Further combining two or more independent Boolean random sets with different intensities and grain properties by forming the intersection and/or union of the sets creates

a great diversity of multi-scale structures with particularly interesting shapes and topologies (see for examples of realisations: Greco et al., 1979; Serra, 1982; Savary et al., 1999; Jeulin, 2000).

Faced with virtually limitless possibilities, finding a combination of BRS that matches a given multi-scale structure is where the difficulty really lies. A model is chosen for its ability to reproduce a finite number of statistical and/or topological properties that can be measured on the observed microstructure. There are several possible properties from which to choose in order to select models that best match given structures and estimate their parameters. Depending on the nature of the model, some of the most used morphological and topological properties include the nearest-neighbour distance function, Ripley's K-function, the pair correlation function (Illian et al., 2008), the variogram (Matheron, 1965), granulometries, which are akin to size distributions (Serra, 1982), the Choquet capacity (Matheron, 1975) and the Euler–Poincaré or connectivity number. In fact, many of these morphological characteristics are correlated. The reader should keep in mind that measurement of these functions is neither always easy nor accurate. For example, much can be said about the measurement of the pair correlation function (Jiao et al., 2007, 2008), whose evaluation is numerically intricate. In order to fully capture the multi-scale nature of the structures of interest, it is also important to achieve unbiased estimation of the abovementioned characteristic functions. This can be made difficult because correlations may exist between measurements at various lags. Many authors use weighted least squares for estimation of model parameters (Pardo-Igúzquiza, 1999). This may not always be advisable and global estimation techniques, such as simulated annealing (Kirkpatrick et al., 1983) or maximum likelihood (Lyman, 2007) are deemed more appropriate by the authors.

A BRS is uniquely defined by its Choquet capacity (Baudin, 1984). The Choquet capacity is analogous to the moments of a probability distribution, except that it is defined in terms of the probability that a given test shape (a compact) will intersect the BRS. In the same way as we can have an effectively infinite number of moments of a probability density, we can have an effectively infinite number of compacts.

The actual number of properties that are considered does not generally exceed three, and this might seem to be hazardous. Matching a number of BRS models, each of which accounts for one scale inside our material, using 3 compacts also could seem adventurous at best. Fortunately, it appears that 2nd order statistics can be sufficient for simulating BRS structures (Aubert and Jeulin, 2000).

This paper is intended as a practical contribution on modelling of multi-scale structures using Boolean random sets. In addition to the potential of such models for creating a wide variety of multi-scale structures, one particularly interesting feature is that a large number of interesting statistical and topological properties have known analytical forms for such models (Serra, 1982). Moreover, from the knowledge about model properties in a given dimension, properties in another dimension can often be predicted. Using BRS models for describing multi-scale structures relies upon union and intersection of BRS models, each individual model capturing a particular scale of the structure. Despite the large number of articles and textbooks about BRS, these are deemed insufficiently explicit to permit non-specialised readers to apply these models to practical problems. By giving all necessary formulae along with an illustrative example, this article aims to form a guide to the use of BRS for modelling multi-scale structures.

2. Basic results for combinations of Boolean random sets through union and intersection

In this section, basic results for combining random closed sets through intersection and union are presented; these results form the bases for modelling multi-scale structures using RACS. Eventually, these results are applied to the special case of Boolean random sets.

RACS have been studied extensively in the field of mathematical morphology pioneered by Matheron (1975). If K describes all possible structuring elements in $\Re^d$, where d is the dimension of space, RACS A is uniquely characterised by its Choquet capacity $T(A,K)$ defined by Serra (1982):

$$T(A, K_x) = P\{K_x \cap A \neq \emptyset\} \tag{1}$$

Subscript x indicates that the spatial location of structuring element K is to be taken into account in the general case. Introducing the functional $\Omega(A, K_x) = P\{K_x \subset A\}$ yields:

$$T(A, K_x) = 1 - P\{K_x \subset A^c\} = 2(1 - q) - \Omega(A, K_x) \tag{2}$$

where A^c is A's complementary set, and q is the Lebesgue fraction of A^c in $\Re^d$. In the general case, the Choquet capacity depends on the actual position x of structuring element K in $\Re^d$. In order to clarify the notations, results presented hereafter are limited to stationary isotropic random sets; hence the location index x is dropped. However, all results can be extended to non-stationary sets by reintroducing position locator x. Given that $T(A,K)$ and $\Omega(A,K)$ are uniquely related through Eq. (2), only functional $\Omega(A,K)$ is used from this point onward for characterising RACS. In particular, when K_x is the doublet $\{x, x+h\}$, functional $\Omega(A,K)$ is equal to the well-known pair correlation function $P\{x \in A; x+h \in A\}$ (Torquato, 2002), also referred to as two-point correlation function (King, 1996). Here, it is noted $\Omega(A,h)$ in the isotropic case. It can be shown that $\Omega(A,K)$ and $\Omega(A^c,K)$ are uniquely related through:

$$\Omega(A, K) = 1 - 2q + \Omega(A^c, K) \tag{3}$$

In the field of mathematical morphology, $\Omega(A^c,h)$ is referred to as the covariance function (Aubert and Jeulin, 2000).

Let us define RACS A as the *intersection* of n mutually independent stationary isotropic RACS A_i, that is $A = \bigcap_{i=1}^{n} A_i$. We have:

$$\Omega\left(\bigcap_{i=1}^{n} A_i, K\right) = P\{K \subset A\} = P\{K \subset A_1\} \times P\{K \subset A_2\} \times \cdots$$

$$\times P\{K \subset A_n\} = \prod_{i=1}^{n} \Omega(A_i, K)$$

So that:

$$\Omega\left(\bigcap_{i=1}^{n} A_i, K\right) = \prod_{i=1}^{n} \Omega(A_i, K) \tag{4}$$

Let us now define q_i and q as the fractions of the complementary sets A_i^c and A^c in $\Re^d$ respectively. Since $\Omega(A^c, K = \{x\}) = q$, Eq. (3) yields: $q = 1 - \prod_{i=1}^{n}(1 - q_i)$.

Contrary to the intersection case, the *union* of n mutually independent stationary isotropic RACS is easily defined using the complementary sets $A^c = \left(\bigcup_{i=1}^n A_i\right)^c = A_1^c \cap A_2^c \cap \cdots \cap A_n^c$. Hence, we have:

$$\Omega(A^c, K) = P\{K \subset A^c\} = P\{K \subset A_1^c\} \times P\{K \subset A_2^c\} \times \cdots \times P\{K \subset A_n^c\}$$

$$= \prod_{i=1}^n \Omega(A_i^c, K)$$

Eq. (3) gives: $q = \prod_{i=1}^n q_i$. Finally, we obtain:

$$\Omega\left(\bigcup_{i=1}^n A_i, K\right) = 1 - 2\prod_{i=1}^n q_i + \prod_{i=1}^n (\Omega(A_i, K) - 1 + 2q_i) \qquad (5)$$

These expressions apply to any types of RACS. In particular, they apply to Boolean random sets. With BRS, the functional $\Omega(A,K)$ is given by (Serra, 1982):

$$\Omega(A, K) = 1 - 2q + e^{-\theta_d \bar{\mu}_d(A' \oplus \breve{K})} = 1 - 2q + e^{\bar{\mu}_d(A' \oplus \breve{K})/\bar{\mu}_d(A')} \qquad (6)$$

where $\bar{\mu}_d(B)$ is the average Lebesgue measure of an element B in $\Re^d$, A' is the primary grain of the BRS, θ_d is the intensity of BRS in $\Re^d$, $\oplus$ is Minkowski addition and $\breve{K}$ is the element K reflected through the origin of the element. The second expression for $\Omega(A,K)$ uses the reduced geometric covariogram $r_d = \bar{\mu}_d(A' \oplus \breve{K})/\bar{\mu}_d(A')$. This expression is particularly interesting for model parameter estimation purposes in that it does not require knowledge of the Boolean process intensity θ_d. This means that calibration of a BRS from functional $\Omega(A,K)$ only involves determining q and the geometric properties of the primary grain A'. Since definition of $\Omega(A,K)$ yields $\Omega(A,\{x\}) = 1 - q$, where $\{x\}$ is a point at an arbitrary location x, θ_d follows from:

$$\theta_d = \frac{1}{\bar{\mu}_d(A')} \ln\left(\frac{1}{q}\right) \qquad (7)$$

We introduce the notation $K_d(h)$ for the geometric covariogram of the BRS' primary grain A' in $\Re^d$, and $r_d(h) = K_d(h)/K_d(0)$ is the primary grain's reduced geometric covariogram in $\Re^d$. Analytical expressions of geometric covariograms are available in the literature for several primary grains, such as discs, spheres, ellipsoids and polyhedra, as well as for distributions of such primary grains (Jeulin, 2000). Then, Eqs. (6) and (7) simplify to Eqs. (8) and (9) respectively:

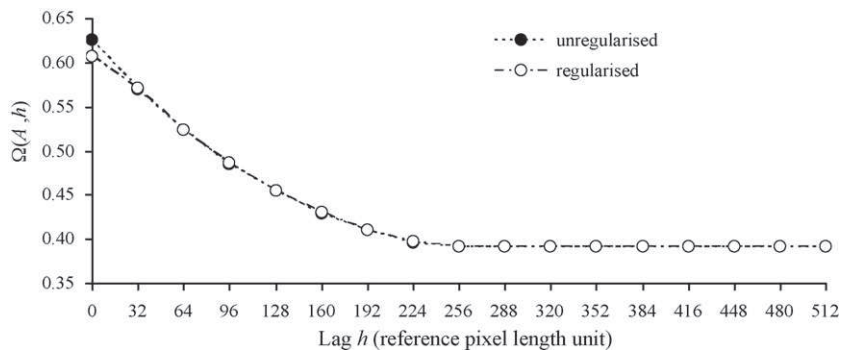$$\Omega(A, h) = 1 - 2q + q^2 e^{\theta_d K_d(h)} = 1 - 2q + q^{2 - r_d(h)} \qquad (8)$$

Fig. 1 – Realisation of a BRS at a chosen reference resolution.

$$\theta_d = \frac{1}{K_d(0)} \ln\left(\frac{1}{q}\right) \qquad (9)$$

Eqs. (6) and (7) in the general case (alt. (8) and (9) in the case of the pair correlation function $\Omega(A,h)$) can readily be substituted into Eqs. (4) and (5) in order to predict functional $\Omega(A,K)$ (alt. functional $\Omega(A,h)$) for any combination of union and intersection of independent stationary isotropic BRS.

The results that have been presented in this section form the basis for quantifying multi-scale structures through combinations of BRS using union and intersection. Such combinations apply to BRS and their complementary sets, recalling that $\Omega(A^c,K)$ and $\Omega(A,K)$ are uniquely related through Eq. (2). An interesting example of combination of BRS and their complementary sets can be found in Greco et al. (1979).

3. Application of combined Boolean random sets to multi-scale materials modelling

Fitting combinations of BRS to multi-scale structures is the purpose of the next section of this paper.

3.1. Boolean random set parameter estimation

Having recalled that functional $\Omega(A,K)$ of any combination of BRS and/or their complementary sets is entirely predictable

Fig. 2 – Example of regularised versus unregularised functional $\Omega(A,h)$.

analytically, the remaining question one may ask is whether it is possible to extract elementary BRS parameters (A', θ_d) from "observed" single- or multi-scale structures.

Firstly, one may wonder whether it is possible to estimate the "true" BRS model parameters directly from the value of functional $\Omega(A,h)$ measured at a given resolution. Indeed, because of pixelisation of the microstructure, one might expect that the resolution of observation of the microstructure may degrade the morphology of the set to the point where BRS parameters can no longer be estimated with pre-
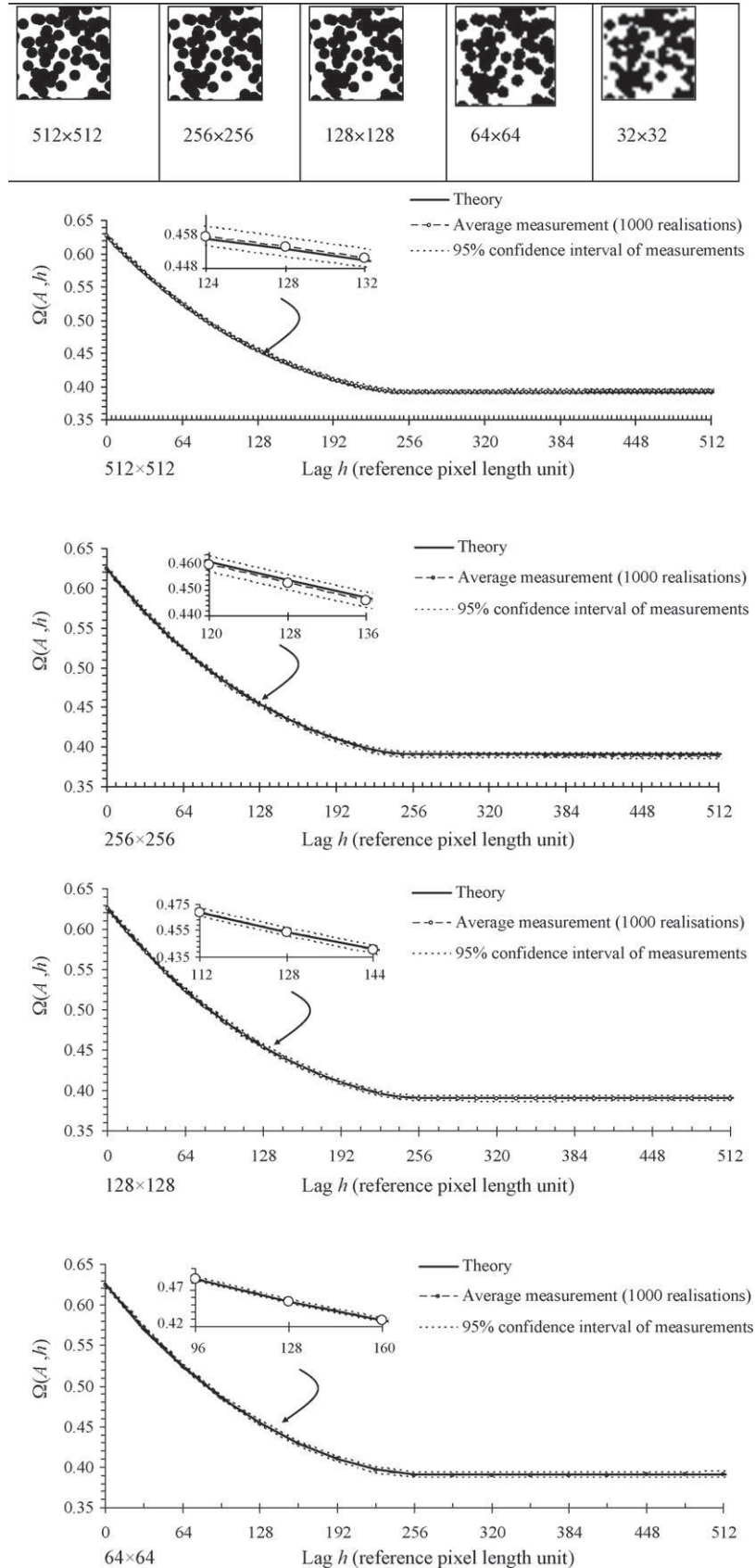

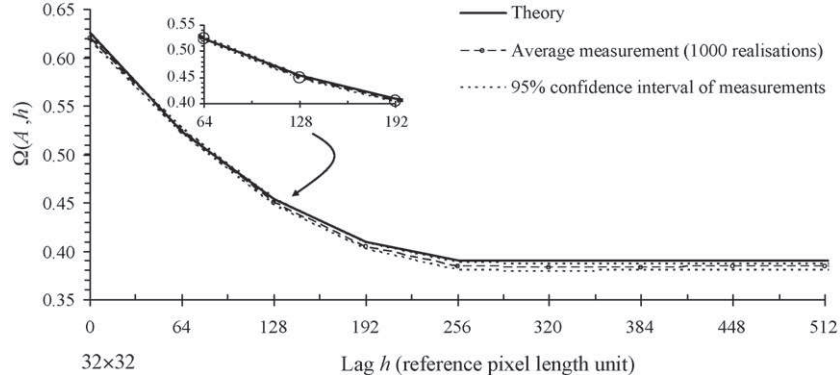Fig. 3 – Effect of resolution on measurement of $\Omega(A,h)$.

Fig. 3 – (Continued)

cision. In order to test this point, let us consider a BRS with monodisperse discs as primary grains. In the unit length of an arbitrary reference pixel length, which we choose to be that of the 2048×2048 sampling resolution, we choose the "true" values of disc diameter and process intensity as $a = 250$ pixels and $\theta = 2 \times 10^{-5}$ per unit area respectively. One realisation of the BRS, generated at the 2048×2048 reference resolution, is shown in Fig. 1.

One thousand (1000) realisations of the BRS were generated at resolutions lower than the reference resolution, from 1024 down to 16 pixels. At every resolution, functional $\Omega(A,h)$ was measured for each realisation and averaged over the 1000 realisations. In each case, realisations were generated at the 2048×2048 resolution using $a = 250$ pixels and $\theta_2 = 2 \times 10^{-5}$; then each realisation was rescaled at a lower resolution using bicubic interpolation. The process of rescaling each realisation requires some care, since it will in the end have bearing on the measurement of functional $\Omega(A,h)$. Two distinct solutions may be used. Starting with a binary image such that of Fig. 1, rescaling to a lower pixel resolution yields a grayscale image, since boundary pixels will combine to give non-binary intensities. The image can then be rebinarised using the appropriate threshold, and the measured functional $\Omega(A,h)$ can be measured on the binary realisation that results. It is interesting to note that the rebinarisation step is not absolutely necessary. Indeed, the theoretical expression for $\Omega(A,h)$ of a rescaled BRS without rebinarisation can be calculated by regularising functional $\Omega(A,h)$ at the reference resolution. If n_1 is the reference pixel resolution (e.g. 2048), and n_2 the rescaled pixel resolution (e.g. 64), then the theoretical expression for $\Omega(A,h)$ at the rescaled resolution can be predicted using Eq. (10):

$$Q_{n_2}(A, h) = \int_{h-0.5(n_1/n_2)}^{h+0.5(n_1/n_2)} \left(\int_{-0.5(n_1/n_2)}^{0.5(n_1/n_2)} Q_{n_1}(A, |w-u|)dw \right) du \quad (10)$$
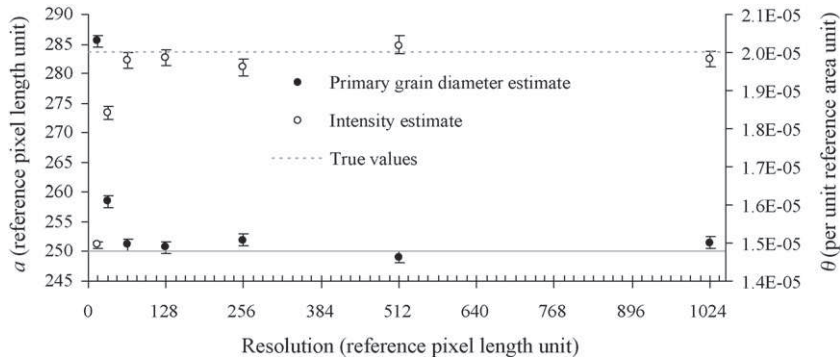
Fig. 2 gives an example of regularised and unregularised $\Omega(A,h)$ for the BRS calculated at the resolution of 64. Having chosen an arbitrary reference resolution of 2048, functional $\Omega(A,h)$ at the 64 resolution gives one value every 32 reference pixel length units. The difference between the 2 theoretical functionals occurs at the origin. In order to estimate BRS parameters from grayscale or rebinarised realisations, one should therefore use the regularised or unregularised expressions for $\Omega(A,h)$ accordingly.

The functional $\Omega(A,h)$ mean value and 95% confidence intervals were measured at each resolution using orthogonal sampling (Jiao et al., 2008) of rebinarised images. As seen from Fig. 3, the measured $\Omega(A,h)$ closely matches the theoretical one down to the 64×64 resolution. Given that the BRS' primary grain is only 7.8 pixels at the 64×64 resolution, this simple test tells us that the morphology of Boolean random sets is particularly well conserved even at low resolution. This observation is quite significant in practice; indeed, it means that BRS parameters can be estimated even from low resolution images of microstructures, which is very interesting from an experimental standpoint. BRS parameter estimation from measured covariance is the object of the next paragraph.

Given the non-linearity of the parameter estimation problem at hand, simulated annealing (Kirkpatrick et al., 1983) is used in this work for BRS parameter estimation. Given a properly chosen cost (or energy) function, such a global parameter estimation technique will yield the global minimum, when other estimation schemes might stop in a local minimum. This work uses the ASAMIN code developed by Sakata (1999), which emulates Lester Ingber's code (Ingber, 1989, 2008) for parameter estimation using Adaptive Simulated Annealing (ASA). The ASA C-code is a fast simulated annealing scheme that uses an exponentially decreasing temperature. The code uses re-annealing and has several tuning options for dealing with

Fig. 4 – Estimation of BRS parameters with ASA as a function of resolution.

many types of non-linear stochastic problems. By combining a variable number of BRS models, the model parameter estimation scheme consists in finding the parameters of the BRS that yield the lowest overall cost. The cost function used here is defined by the weighted sum of squares of residuals given by Eq. (11):

$$\text{cost} = \sum_{h=1}^{n\,\dim/2} w(h) \times \left(\Omega(A, h) - \hat{\Omega}(A, h) \right)^2 \qquad (11)$$

Reflecting the relative number of times lag h can be placed onto the image when $\Omega(A,h)$ is measured using orthogonal sampling (Jiao et al., 2008), this work uses the following weights $w(h)$ for estimating BRS parameters from an image of length $n\,\dim$:

$$w(h) = n\,\dim - h \qquad (12)$$

The ASA algorithm was used to estimate the BRS parameters from function $\Omega(A,h)$ measured at the abovementioned resolutions. Fig. 4 shows the estimated BRS parameters as a function of sampling resolution and their 95% confidence intervals.

From the above results, it can be concluded that the ASA parameter estimation scheme is a suitable scheme for estimating BRS parameters from functional $\Omega(A,h)$ measurements. As expected from the earlier observations, this simple numerical example confirms that provided resolution is not too low with respect to the primary grain size, resolution does not affect the precision or the accuracy of the parameter estimation for BRS.

3.2. Parameter estimation for combined Boolean random sets

Having discussed some of the practical questions of parameter estimation for a single BRS, the ASA parameter estimation scheme was applied to known BRS combined through intersection. Firstly, the target value for $\Omega(A,h)$ was taken as the theoretical value for the intersection of 4 BRS whose parameters are given in Table 1. The parameters are given in reference pixel length unit from a 1024×1024 reference resolution. As shown in Fig. 5, which displays a realisation of the combined BRS, the combination of these BRS truly yields a multi-scale microstructure.

Since the ASA scheme is tested against the theoretical functional $\Omega(A,h)$, the cost function is defined using unweighted Eq. (13) rather than Eq. (11):

$$\text{cost} = \sum_{h=1}^{n\,\dim/2} \left(\Omega(A, h) - \hat{\Omega}(A, h) \right)^2 \qquad (13)$$
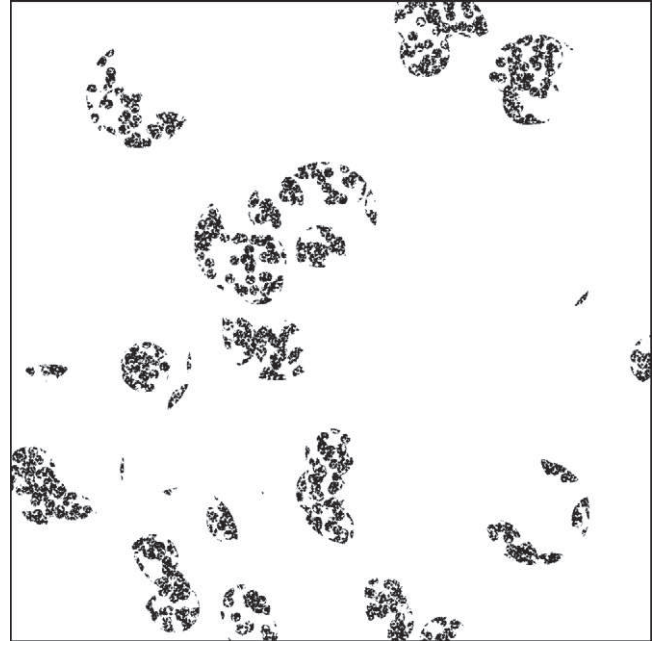

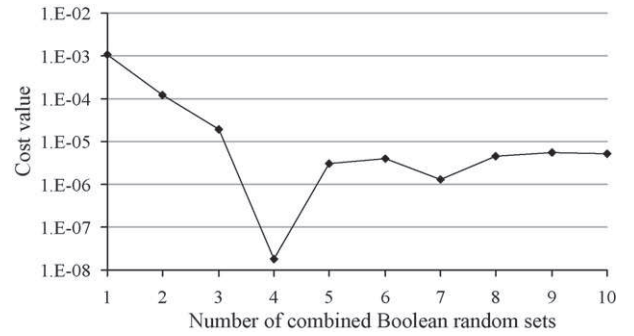**Fig. 5 – Realisation of the combined BRS example (parameters are given in Table 1).**

Fig. 6 – Variation of the cost function with increasing number of BRS.

Fig. 6 shows the variation of the cost function that was obtained as the number of combined BRS – with monodisperse discs as primary grains – is increased from 1 to 10. The ASA parameter estimation algorithm is able to identify a clear minimum which corresponds to the combination of exactly 4 BRS. The estimated BRS parameters are given in Table 1 in the two right-hand side columns. The agreement between actual and estimated parameters proves that the ASA algorithm is able to recover the right combination of BRS accurately.

Having established that the ASA estimation scheme can successfully estimate combined BRS parameters from theoretical functional $\Omega(A,h)$, we can now assess the ASA scheme against $\Omega(A,h)$ measured from realisations of combined BRS. Because combined BRS in effect yield multi-scale microstruc-

Table 1 – Test of ASA algorithm for estimation of combined BRS parameters.				
BRS A_i	Parameters of 4 independent stationary isotropic BRS using monodisperse discs as primary grains		Estimated parameters using ASA	
	θ_{2i} number of discs/unit surface area	a_i disc diameter (pixel)	$\hat{\theta}_{2i}$	$\hat{a}_i$
A_1	1×10^{-5}	170	9.95×10^{-6}	168.70
A_2	1×10^{-4}	80	1.04×10^{-4}	79.20
A_3	5×10^{-3}	16	5.08×10^{-3}	15.89
A_4	1×10^{-1}	4	1.01×10^{-1}	3.99
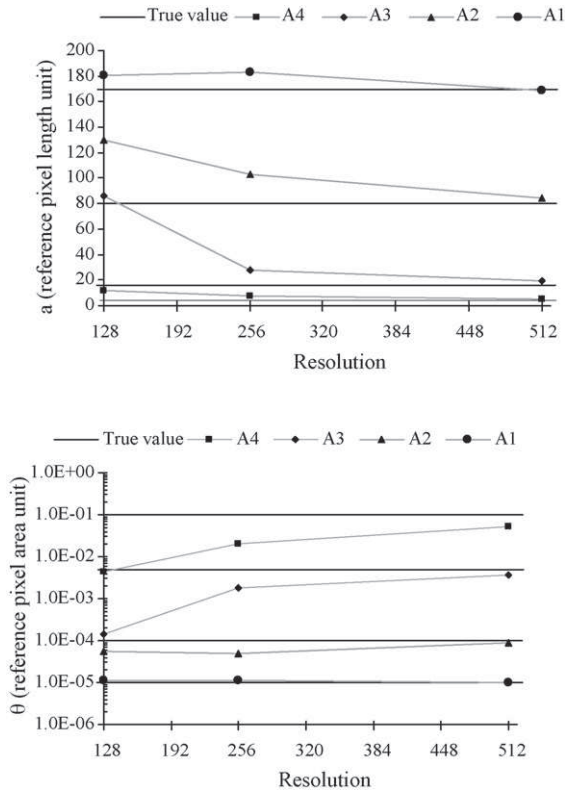
Fig. 7 – Parameter estimates as a function of resolution for combined BRS.

tures, the problem of pixel resolution and image size becomes critical. If the resolution is lower than the characteristic size of a given random set present in the microstructure, it goes without saying that it will not be possible to estimate the corresponding BRS parameters accurately. If the image size is insufficient, the random sets with the largest characteristic dimension may not be sampled in a representative manner; hence it will not be possible to estimate its parameters accurately. Surely, these issues could be circumvented provided large high resolution images are available. In practice, one is often faced with limitations on available combinations of image size and pixel resolution. As an illustrative example, 100 realisations of the combined BRS of Table 1 were generated at different pixel resolutions: 512×512, 256×256, 128×128, and 64×64. Combined BRS parameters were estimated using ASA for the average measure of $\Omega(A,h)$ at each resolution. The parameter estimates are plotted in Fig. 7 as a function of resolution.
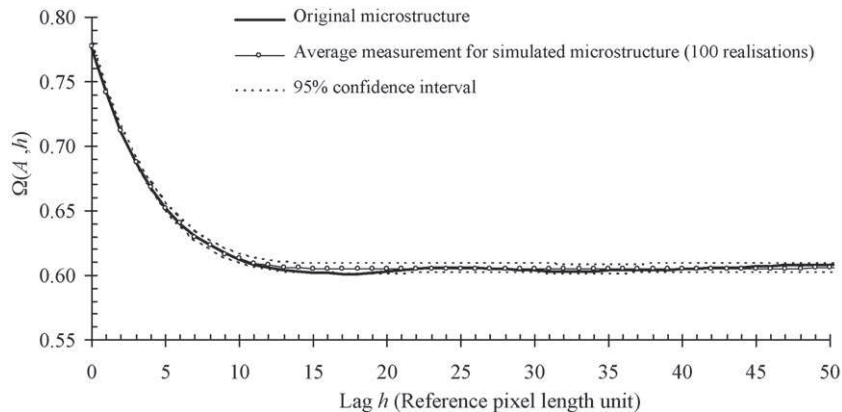
As expected, we observe that the combination of estimated BRS parameters becomes closer to its true value as resolution is increased. This result is in fact a simple consequence of the fact that the measured $\Omega(A,h)$ becomes closer to the theoretical value as resolution increases. In our example, we find that the ASA scheme is able to estimate the correct combination of parameters for all 4 BRS at a 512×512 resolution; however, it does not give satisfactory results at the 256×256 resolution. The smallest primary grain being a 4 pixel diameter disc at the 1024×1024 reference resolution, this yields 2 pixel diameter discs at the 512×512 resolution. From this simple observation, one may conclude as a practical rule that the lowest resolution for BRS parameter estimation should be such that one pixel is equal to the size of the smallest physical feature one wishes to observe.

Our results thus far have enabled us to review some key practical building blocks for matching a combination of Boolean random sets to two-dimensional binary images of multi-scale microstructures:

- Functional $\Omega(A,h)$ for any combination of BRS through union and intersection is entirely predictable analytically through Eqs. (4) and (5).
- The ASA parameter estimation scheme is suitable for estimating parameters of combined BRS from measured functional $\Omega(A,h)$.
- The cost function given by Eqs. (10) and (11) is satisfactory for identifying the best combination of BRS.
- Given the sensitivity of combined BRS parameter estimation to pixel resolution, pixel length should be no greater than the size of the smallest microstructural feature or scale one wishes to characterise.

With this in mind, we are now in a position to apply the proposed combined BRS parameter estimation scheme to real microstructures.

3.3. Modelling real microstructures with combined BRS

Fig. 8 shows a binarised cross-section image of Berea permeable sandstone published by Dullien (1992). We shall assume that this image corresponds to a plane taken at random through a three-dimensional isotropic structure. Clearly, there is no relevance in attempting to fit BRS with two-dimensional primary grains to a cross-section image through a three-dimensional microstructure. Although a great variety of three-dimensional primary grains can be used, we

Fig. 8 – Measurement of functional $\Omega(A,h)$ for original and simulated microstructures.
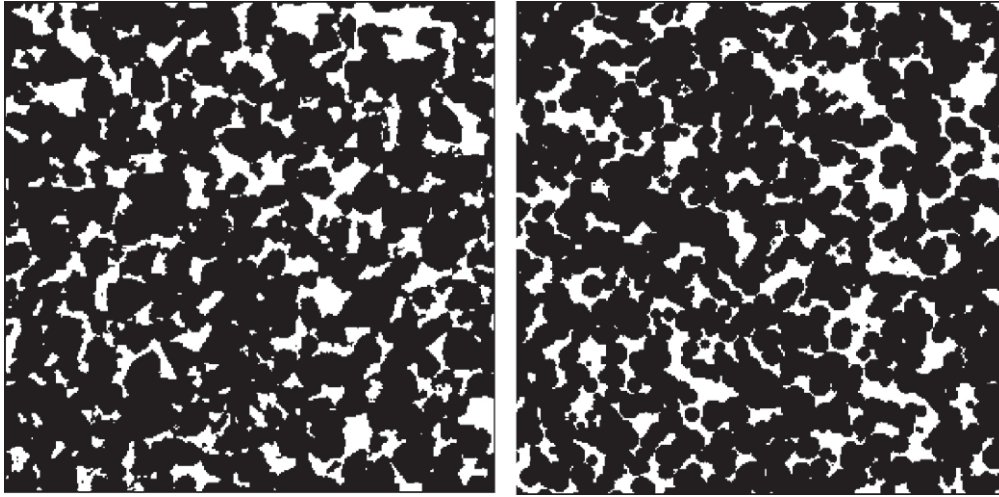
Fig. 9 – Visual comparison between original microstructure (left) and simulated microstructure using estimated BRS parameters (right).

shall restrict our application of the above results to BRS with spheres as primary grains. Amongst the standard diameter size distributions that can be used, we limit the parameter estimation exercise to 3 sphere diameter distributions: monodisperse, uniform and linear. The ASA parameter estimation scheme returned 2 solutions that yielded the lowest cost value overall:

- 5 BRS with monodisperse spheres as primary grains. The estimated diameters and process intensities are $a = (13.8; 18.2; 20.3; 27.9; 33.3)$ pixels and $\theta_3 = (0.00116; 0.00126; 0.00110; 0.00059; 0.00038)$ spheres per unit volume respectively.
- 1 BRS with a linear diameter distribution of spheres as primary grains. The estimated maximum diameter of the spheres and process intensity are $a = 15.823$ pixels and $\theta_3 = 1.813 \times 10^{-3}$ spheres per unit volume respectively.

Here, the values of the parameters are given in the pixel length unit of the original image. One hundred realisations of the fitted BRS were generated, and the average function $\Omega(A,h)$ is plotted in Fig. 8 with the value measured on the original sandstone image. The agreement between the two confirms of the effectiveness of the BRS parameter estimation scheme proposed in this work.

A random cross-section taken through a three-dimensional realisation of the estimated BRS with linearly distributed parameters ($a = 15.823$; $\theta_3 = 1.813 \times 10^{-3}$) is shown in Fig. 9. Its visual similarity to the sandstone image gives an indirect confirmation of the BRS parameter estimates. In practice, as the eye is sensitive to small morphological differences, such as the difference between the slightly angular grains in the original structure and the roundness of the spheres used with the BRS, a good practical way for comparing original and simulated microstructures visually is to look at them side-by-side slightly out of focus. A distribution of angular primary grains, such as Poisson polyhedra for example might possibly give even better results in this particular case.

The fitted BRS being three-dimensional, the estimated parameters readily permit reconstruction of the sandstone microstructure in three dimensions. As indicated earlier, the simulated cross-section of Fig. 9 was in fact taken as a random cross-section through a three-dimensional realisation of the estimated BRS. The left-hand side image of Fig. 10 shows a three-dimensional realisation of the estimated BRS, whereas the right-hand side image shows the corresponding pore space.

Overall, the microstructure fitting procedure described in this paper provides straightforward implementation tools for simulating three-dimensional microstructures from two-
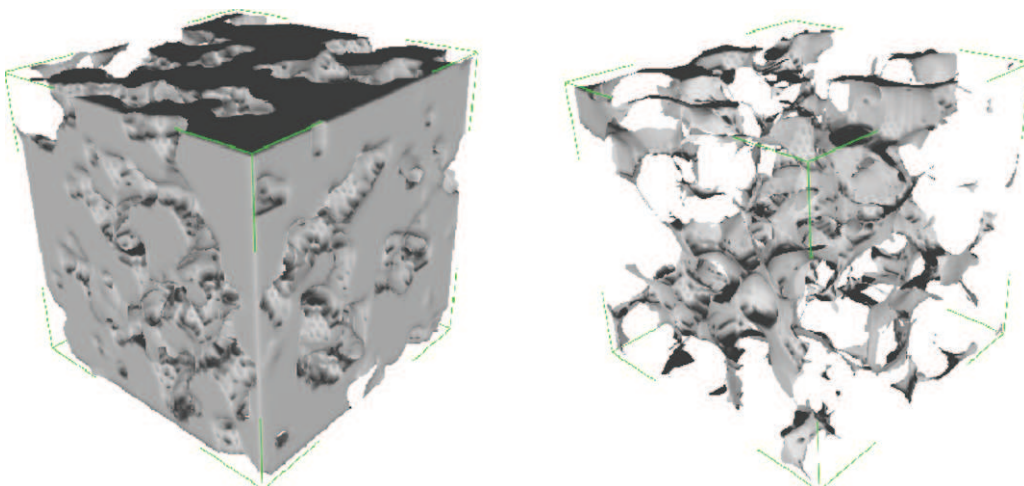
Fig. 10 – Three-dimensional simulation of Berea sandstone using estimated BRS parameters.

dimensional observations using combinations of BRS. From a materials analysis viewpoint, this approach is quite powerful. Because one is able to generate a limitless number of realisations of the three-dimensional microstructure from the estimated BRS, combined BRS give material scientists and engineers the possibility of seeking and obtaining statistically robust results about the relationship between morphological/topological properties of the microstructure and the properties in service. For example, a realisation such as Fig. 10, which can be generated in a matter of seconds, can be poured into a fluid flow simulation package for analysis of its transport properties. Moreover, important topological properties such as the Euler–Poincaré number can be derived analytically from BRS parameters (Miles, 1976). The possibility of deriving topological results analytically from combined BRS is another significant strength of using combinations of BRS to describe real microstructures.

This paper has presented elementary and easily implementable results and procedures for fitting combinations of BRS to microstructures. These practical tools are sufficient for anyone who wishes to start quantifying a material structure using BRS. Nevertheless, several issues of practical significance were not addressed in the present paper. These are:

- The cost function that has been used in this work relies solely on functional $\Omega(A,h)$. Such a function may not be sufficient to differentiate between closely related combinations of BRS. Evidence of this can be found in the results presented earlier. Indeed, amongst the three types of BRS that were used to fit the sandstone microstructure example, the ASA parameter estimation scheme returned the same lowest cost value for both a combination of 5 BRS with monodisperse spheres and a single BRS with linearly distributed spheres. Additional functionals, such as the three-point functional $\Omega(A,h_1,h_2)$ (Aubert and Jeulin, 2000) can be added into the cost function in order to make finer distinctions between BRS.
- With the sole objective of testing the proposed combined BRS parameter estimation scheme, the parameter estimation exercise for the sandstone microstructure was intentionally limited to combinations of 3 possible BRS through intersection. Moreover, no allowance was made for combining BRS of different types. In practice, it is natural to want to test a greater number of possible combinations. One must be aware of the fact that the space of possible combinations is virtually infinite. Indeed, it depends on the types of BRS one may consider, the number of BRS used in a combination, the phase of the BRS that is used (A or A^c), and finally, the nature and order of the combination (union and intersection). In the end, one ought to restrict the search to a limited number of possible combinations; otherwise the problem will become overwhelming. Observation of the microstructure of interest is a fundamental prerequisite for orientating the choice of possible BRS and the way they might be combined.
- The results and methods presented in this paper can readily be used to estimate three-dimensional BRS parameters not only from cross-sections, but also from volume images of microstructure (e.g. tomographic images). Where tomographic measurements can only yield a few images of a microstructure of interest because of time and cost issues, estimation of combined BRS from volume images can simulate as many realisations of the microstructure as required. Hence, the authors are of the opinion that microstructure

modelling using spatial statistics, such as described in this paper for instance, remains an invaluable companion for tomographic imaging work.
- Not all microstructures can be described using combinations of BRS. There exist a number of techniques that may help decide whether BRS can possibly render a given microstructure. The reader is invited to review Serra's classic textbook (Serra, 1982), which contains several pointers about this important issue. The central question is what is it that one wants to achieve by matching a combination of BRS to an observed microstructure. For example, if we are interested in the general connectivity of a given material phase inside a microstructure, like with pores for instance, it may not be necessary to seek a model that captures all the details of that particular phase. If this is the case, then one is likely to find a relatively simple combination of BRS that will describe the texture satisfactorily, even though it is not capable of describing all the textural details. In this sense, the results presented in this paper have a wide range of applicability.

4.   Conclusions

Boolean random sets have powerful morphological and topological properties. Moreover, they can be combined in any number of ways to produce a very wide variety of microstructures. Based on well-established theory of BRS, this paper reviews elementary applied notions about combination of BRS, with the objective of providing material scientists and engineers with results they can readily apply to their own analyses of materials. The work proposes and validates a reliable solution for estimating combined BRS parameters through intersection and union, from the covariance function measured on images of microstructure. Using a stepwise approach that starts from the simplest BRS to combinations of BRS, this work shows that Adaptive Simulated Annealing is able to recover BRS parameters efficiently using a simple cost function. Various issues related to parameter estimation from images, such as pixel resolution, are also discussed in a practical sense. It is found that BRS are well conserved as pixel resolution decreases, which is a strong argument in favour of using such models for describing multi-scale microstructures. Finally, the proposed combined BRS parameter estimation scheme is applied to a real case situation; it is able to estimate BRS that yield convincing realisations of the observed microstructure in two and three dimensions.

References

Aubert, A. and Jeulin, D., 2000, Estimation of the influence of second- and third-order moments on random sets reconstructions. Pattern Recognition, 33: 1083–1104.

Baudin, M., 1984, Multidimensional point processes and random closed sets. Journal of Applied Probability, 21: 173–178.

Cressie, N.A.C., (1993). *Statistics for Spatial Data Revised Edition (Wiley Series in Probability and Mathematical Statistics)*. (John Wiley & Sons, Inc).

Cuzick, J. and Edwards, R., 1990, Spatial clustering for inhomogeneous populations (with discussion). Journal of the Royal Statistical Society, Series B, 52: 73–104.

Diggle, P.J., (1983). *Statistical Analysis of Spatial Point Patterns*. (Academic Press, New York).

Dullien, F.A.L., (1992). *Porous Media: Fluid Transport and Pore Structure* (Second ed.). (Academic Press, New York).

Greco, A., Jeulin, D. and Serra, J., 1979, The use of the texture analyser to study sinter structure. Journal of Microscopy, 116(2): 199–211.

Illian, J., Penttinen, A., Stoyan, H. and Stoyan, D., (2008). *Statistical Analysis and Modelling of Spatial Point Processes, Statistics in Practice Series*. (John Wiley & Sons Ltd, UK).

Ingber, L., 1989. Mathematical and computer modelling 12, pp. 969–973.

Ingber, L., 2008. Adaptive simulated annealing (ASA). Lester Ingber Research, McLean, VA, (The source code for the ASA algorithm is available at www.ingber.com).

Jeulin, D. and Moreau, M., 2005, Multi-scale simulation of random spheres aggregates—application to nanocomposites, In *Proceedings of the 9th European Congress of Stereology* Zakopane, Poland, May 10–13, , pp. 341–348.

Jeulin, D., 2005, Bilodeau, M., Meyer, F., & Schmitt, M. (Eds.), *Random Structures in Physics, in Space, Structure, and Randomness, Contributions in Honour of Georges Matheron in the Fields of Geostatistics, Random Sets, and Mathematical Morphology; Series: Lecture Notes in Statistics* , pp. 183–222.

Jeulin, D., 2000, Random texture models for material structures. Statistics and Computing, 10: 121–132.

Jiao, Y., Stillinger, F.H. and Torquato, S., 2007, Modeling heterogeneous materials via two-point correlation functions: basic principles. Physical Review E, 76: 031110-1–031110-15.

Jiao, Y., Stillinger, F.H. and Torquato, S., 2008, Modeling heterogeneous materials via two-point correlation functions. II. Algorithmic details and applications. Physical Review E, 77: 031135-1–031135-15.

King, R.P., 1996, Random geometrical models for porous media and other two-phase materials. The Chemical Engineering Journal, 62: 1–12.

Kirkpatrick, S., Gelatt, C.D. and Vecchi, M.P., 1983, Optimization by simulated annealing. Science, 220(4598): 671–680.

Lyman, G., 2007, Optimal sampling for variogram estimation, In *Third World Conference on Sampling and Blending* Porto Alegre, Brasil, October 2007, Fundacao Luiz Englert, Porto Alegre,

Matheron, G., (1975). *Random Sets and Integral Geometry*. (Wiley, New York).

Matheron, G., (1965). *Les variables régionalisées et leur estimation*. (Masson, Paris).

Miles, R.E., 1976, Estimating aggregate and overall characteristics from thick sections by transmission microscopy. Journal of Microscopy, 107: 227–233.

Møller, J., 2005, Properties of spatial Cox process models. Journal of Statistical Research of Iran, 2: 1–18.

Pardo-Igúzquiza, E., 1999, VARFIT: a fortran-77 program for fitting variogram models by weighted least squares. Computers & Geosciences, 25: 251–261.

Rataj, J. and Saxl, I., 1997, Boolean cluster models: mean cluster dilations and spherical contact distances. Mathematica Bohemica, 1: 21–36.

Sakata, S., (1999). *ASAMIN—A MATLAB Gateway to Lester Ingber's Adaptive Simulated Annealing Software (Software)*. (University of Michigan, Ann Arbor, MI). Available at: http://www.econ.ubc.ca/ssakata/public_html/software/

Savary, L., Jeulin, D. and Thorel, A., 1999, Morphological analysis of carbon–polymer composite materials from thick sections. Acta Stereologica, 18(3): 297–303.

Serra, J., (1982). *Image Analysis and Mathematical Morphology*. (Academic Press).

Stoyan, D., 1992, Statistical estimation of model parameters from planar Neyman–Scott cluster processes. Metrika, 39: 67–74.

Torquato, S., (2002). *Random Heterogenous Materials: Microstructure and Macroscopic Properties*. (Springer–Verlag, New York).